Core-level spectroscopy study of the Li/Si(111)-3×1, Na/Si(111)-3×1, and K/Si(111)-3×1 surfaces

M. Gurnett, J. B. Gustafsson, L. J. Holleboom, K. O. Magnusson, S. M. Widstrand, and L. S. O. Johansson*
Department of Physics, Karlstad University, SE-651 88 Karlstad, Sweden

M. K.-J. Johansson and S. M. Gray
Department of Synchrotron Radiation Research, Institute of Physics, Lund University, P.O. Box 118, SE-221 00 Lund, Sweden
(Received 18 January 2004; revised manuscript received 1 February 2005; published 19 May 2005)

In this article we report Si 2*p* core-level spectroscopy results from the alkali (Li, Na, and K) induced Si(111)-3×1 reconstructions. The experimental results are compared to the theoretical honeycomb-chain channel (HCC) model for the 3×1 reconstruction using density functional theory (DFT) to calculate core-level shifts using both initial and final-state calculation schemes. Si 2*p* core-level spectra for the Li, Na, and K reconstructions showed two surface related components lying on either side of the main bulk Si $2p_{3/2}$ peak. An additional higher binding energy component was found for K. All core-level spectra showed strong similarities leading to the conclusion that the surfaces do indeed share a common structure. With increasing alkali metal size, the lower binding energy component was found to shift away from the main bulk peak. Our theoretical calculations also show a similar trend. It is concluded that the lower binding energy surface component originates from the alkali atom bonded Si atoms. The origin of the higher binding energy component was determined based on trends in the peak height and final-state DFT calculations. It was found that this component derives from several atoms in the first and second layers. Calculations which include final-state effects were found to be in good agreement with the experimentally determined surface core-level shifts.

DOI: 10.1103/PhysRevB.71.195408 PACS number(s): 73.20.At, 79.60.Dp

I. INTRODUCTION

The alkali metal induced reconstructions on Si surfaces have long been of interest due to their believed simple bonding configuration, making them ideal as model systems. One of these reconstructions is the *M*/Si(111)-3×1 reconstruction for *M*=Li, Na, K, and Cs. This reconstruction is also formed for *M*=Mg, Ba, Ca, and Ag. Over the years a number of structural models have been proposed for this reconstruction including both the extended Pandey-chain (EPC) (Ref. 1) and the Seiwatz-chain model,[2,3] neither of which showed good agreement with valence band photoemission measurements. To date, the honeycomb chain-channel model proposed by Collazo-Davillo, Grozca, and Marks[4] and independently by Lottermoser *et al.*[5] has shown greatest promise. This result was based on work done using a combination of experimental surface x-ray diffraction (SRXD), low energy electron diffraction (LEED) and density functional theory (DFT) calculations for the Li/Si(111)-3×1 reconstruction and on comparisons between calculations and valence band spectra. Initially this model was denoted by Lottermoser *et al.* as the 560560 or 650650 depending on the Si atom responsible for bonding with the surface alkali metal adatom. It will, however, be referred to here as the honeycomb chain-channel (or HCC) model, as proposed by Erwin and Weitering.[6] First principles calculations for the Li/Si(111)-3×1 reconstruction performed by Erwin and Weitering[6] have shown this model to have the lowest energy of all models proposed thus far. Similar DFT calculations for the Na/Si(111)-3×1 reconstruction have been carried out by Kang, Kang, and Jeong.[7]

Of further interest is the belief that the same 3×1 reconstruction as that induced by the alkali metals on Si(111) is also formed for Ag,[8,9] Ca,[10] Mg, and Ba (Refs. 11–13 on Si(111) as well as for the alkali induced Ge(111)-3×1 reconstruction.[14]

One of the more interesting details of this model is the inclusion of a Si double bond located on the top layer. A one-dimensional channel is formed in the $[\bar{1}10]$ direction, in which one adatom per 3×1 unit cell (1/3 monolayer) is located in the first layer.

The electronic structure of the *M*/3×1 surfaces have been studied by angle-resolved photoemission (ARUPS) for the cases of Na,[15] Mg,[16] K,[17] and Ag.[8,9] A previous core-level study of the Li/Si(111)-3×1 surface has been presented by Weitering, Shi, and Erwin.[18] and core-level measurements on the Na/Si(111)-3×1 surface have been performed previously by Okuda *et al.*[19] and Paggel *et al.*[20,21] We have recently studied the Ag/Si(111)-3×1/6×1 reconstruction[9] by means of angle-resolved photoelectron spectroscopy in which experimental band structures taken in the $\bar{\Gamma}$-$\bar{K}$ and $\bar{\Gamma}$-$\bar{M}$ directions were found to show good agreement with calculated band maps for the HCC model.

In the following article we present our findings on high resolution surface core-level shifts of the alkali (Li, Na, and K) induced Si(111)-3×1 reconstructions. Comparisons are then made with DFT calculations of the surface core-level shifts performed using both initial and final-state schemes.

II. EXPERIMENTAL DETAILS

Measurements were performed at the MAX-lab national synchrotron radiation laboratory in Lund, Sweden. All measurements, with the exception of Li/Si(111)-3×1, were per-

formed at beamline 33.[22] This beamline is equipped with a large spherical grating monochromator, which allows for photon energies ranging between 15 and 200 eV. An ARUPS10 angular resolved electron energy analyzer from VG Microtech and low energy electron diffraction (LEED) optics are both incorporated in the end station. The base pressure in the analyzer chamber during the experiments was less than 1×10^{-10} mbar during the K and Na experiments.

Measurements on Li/Si(111)-3×1 were performed at beamline 22. This beamline was equipped with a modified SX-700 monochromator yielding a highly monochromatic photon beam in the UV (ultraviolet) and soft x-ray range. The end station of this beamline was built up around a large hemispherical Scienta electron analyzer. The base pressure was less than 1×10^{-10} mbar.

Energy resolutions were of the order of 85 meV for a photon energy of 130 eV for the measurements performed on the Li/Si(111)-3×1 at beamline 22. A total energy resolution of around 100 meV at a photon energy of 130 eV was used at beamline 33.

The sample used for all measurements with the exception of Li was an *n*-type (phosphorous doped) $\rho=0.01-0.02\ \Omega$ cm Shiraki etched[23] vicinal Si(111) 5×15 mm wafer with a thickness of 300 μm. The misorientation of the crystal was 2 ± 0.5 in the $[11\bar{2}]$ crystallographic direction. The reason for the use of a vicinal sample was an attempt to obtain a single domain reconstruction in order to simplify analysis of valence band maps. This was, however, not achieved in this case. Single domain 3×1 reconstructions have previously been studied for Mg by An *et al.*,[16] Ca by Petrovykh *et al.*,[24] Gallus *et al.*,[25] and Kim *et al.*,[26] Ba by Okuda *et al.*[11] and Schäfer *et al.*,[13] and in our previous study of the Ag/Si(111)-$3\times1/6\times1$ reconstruction.[9] The sample used in the case of the Li measurements was a medium *n*-doped Shiraki etched Si(111) wafer.

The samples were outgassed in the ultrahigh vacuum (UHV) chambers for several hours at about 600 °C by means of direct current heating. A good-quality clean 7×7 surface was obtained after several minutes of annealing at 900 °C. In the Li/Si(111) experiment, the 7×7 surface was obtained by several flash heatings to 1175 °C. During the experiment, surface temperatures were measured by means of an infrared pyrometer.

The alkali metals were deposited by means of well outgassed alkali metal dispensers from SAES Getters S.p.A. at a distance of a few centimetres from the sample. Before each alkali deposition, the quality of the 7×7 sample surface was checked using both LEED and photoemission spectra.

III. COMPUTATIONAL DETAILS

Density functional theory (DFT) calculations were performed using the full-potential linear augmented plane wave with local orbitals method (FP-LAPW+lo) as implemented in WIEN2K[27] using the general gradient approximation (GGA) exchange-correlation potential of Perdew, Burke, and Ernzerhof.[28]

This method solves the Kohn-Sham equations by separating regions in space into non-overlapping atomic spheres and interstitial regions. The size of the atomic spheres is specified by the muffin tin radius, R_{mt}. Inside the atomic sphere a basis set comprised of a linear combination of radial functions multiplied by spherical harmonics is used. In the interstitial region a plane wave basis is used.

The three systems were modeled using a periodic slab geometry consisting of 12 Si layers separated by a 18 Å vacuum gap. The slab itself was mirrored in the *xy* plane halfway along the [111] direction (spacegroup 6*pm*). A single adatom was placed on either side of the slab, thus allowing for the formation of the reconstruction on both sides of the slab. All atoms with the exception of the two single layers that lie on either side of the mirror plane were allowed to relax through total energy minimization until the individual

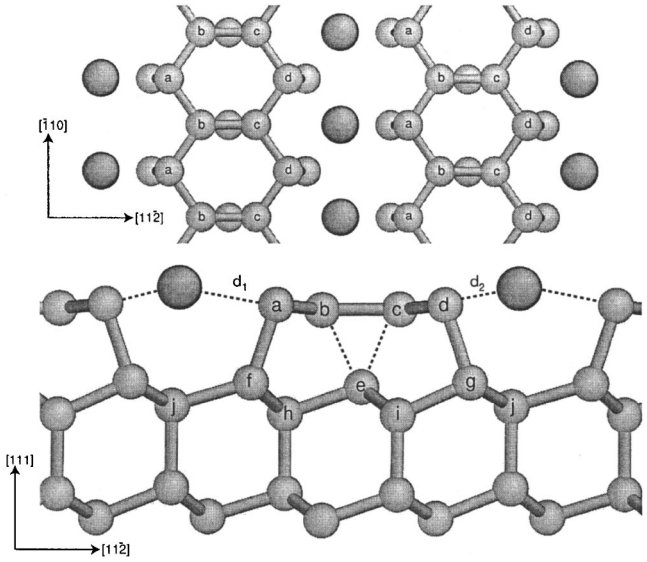

FIG. 1. Honeycomb chain-channel model for the alkali metal induced Si(111)-3×1 reconstructions (Ref. 30). The adatoms (indicated by darker spheres) are located in a 1D channel which travels along the $[\bar{1}10]$ direction. The formation of a double bond between Si atoms *b* and *c* is also included in the model. The choice of notation is the same as for Ref. 10.

TABLE I. Assorted distances (in Å) for the Li/Si(111)-3×1, Na/Si(111)-3×1, and K/Si(111)-3×1 reconstructions. Also included are the 1×1 Si bulk unit cell parameters and that of the 3×1 slab.

Si(111)-1×1 (hexagonal)										
	a	b	c	α	β	γ				
	3.86	3.86	9.49	90°	90°	120°				
M/Si(111)-3×1 slab (space group 6pm)										
	a	b	c[a]	α	β	γ	V_g			
	10.21	3.86	52.86	90°	90°	100.89°	18			
M		d_1	d_2	d_{ab}	d_{bc}	d_{cd}	d_{be}	d_{ce}	d_{af}	d_{dg}
Li		2.77	2.93	2.38	2.33	2.38	2.59	2.60	2.44	2.42
Na		2.90	2.96	2.36	2.30	2.36	2.58	2.58	2.44	2.42
Na[b]		2.95	3.05	2.38	2.31	2.38	2.59	2.59	2.45	2.44
K		3.19	3.22	2.35	2.28	2.35	2.58	2.57	2.43	2.42

[a]This value includes the vacuum gap, V_g.
[b]Na values are the distances found in Ref. 14.

force components on any given atom was no greater than 1 mRyd/Å. The resulting geometry of the surfaces for the Li, Na, and K induced Si(111)-3×1 reconstructions can be seen in Fig. 1. A muffin tin radius of 2 a.u. was used for the Si, Li, Na, and K atoms. An energy cut-off of −6 Rydberg was used to separate core and valence states. A plane wave cut-off of 85 eV ($R_{\mathrm{mt}}K_{\mathrm{max}}=5$) was used with 12 **k** points in the irreducible Brillouin zone. Local orbitals were added to improve calculations. Volume optimization of a hexagonal Si(111) unit cell resulted in an Si—Si bulk bond length of 2.365 Å. This compares fairly well with the experimental values of 2.33 Å and that calculated by Kang, Kang, and Jeong[7] (2.38 Å). Various distances for the three reconstructions together with a comparison to previously reported distances, as calculated by Kang, Kang, and Jeong[7] for the Na/Si(111)-3×1 reconstruction, can be found in Table I. These lengths are found to be in good agreement, especially when one takes into account the differences in the bulk bond lengths between the calculations.

Surface core-level shifts (SCLS) were calculated using two different schemes. Initial state core-level shifts are found by determining the difference in the Kohn-Sham energy eigenvalues between the surface and bulk atoms. However, calculations of this type neglect the formation of core-holes and their effect on the surrounding atoms due to screening. These effects can lead to relatively large changes in the shifts from those obtained from initial state core-level calculations. With the introduction of so-called Slater-Janak transition states[29] it is possible to model, to some degree, final-state effects. In this approach, the occupation number for a given state and atom is reduced by 0.5 and then reintroduced as background so as to maintain a neutral system. The self-consistent field (SCF) procedure is then run as usual until the calculations are well converged. This procedure is then repeated until all atoms of interest have been processed. Using this scheme we obtain core-level shifts that include both initial and final-state effect contributions.

In order to include final-state effects, the 3×1 unit cell size was doubled in the $[\bar{1}10]$ direction. This is done so as to separate the ionized atoms, which was found to be important for an accurate determination of the bulk reference energy.

IV. EXPERIMENTAL RESULTS AND ANALYSIS

The following subsections contain the resulting experimental core-level data and fits obtained for the M/Si(111)-3×1 reconstructions for M=Li, Na, and K. Spectra were taken at various photon energies, $h\nu$, so as to obtain both bulk and surface sensitive core-level spectra. The more surface sensitive measurements are found to occur at

TABLE II. Parameters used to fit the experimental Si 2p core-level data for the Li, Na, and K induced Si(111)-3×1 reconstructions. The Lorentzian FWHM, was set to 85 meV for all fits. The spin-orbit split was approximately 0.607 eV for all fits performed. Branching ratios were allowed to vary between 0.45 and 0.55. The binding energies are relative to the bulk component in each case.

	Binding energy shift (eV)	Gaussian FWHM (meV)
Li/Si(111)-3×1		
Bulk		247
S_1	−0.36	332
S_2	0.22	368
Na/Si(111)-3×1		
Bulk		248
S_1	−0.40	290
S_2	0.24	294
K/Si(111)-3×1		
Bulk		324
S_1	−0.57	362
S_2	0.25	384
S_3	0.57	396

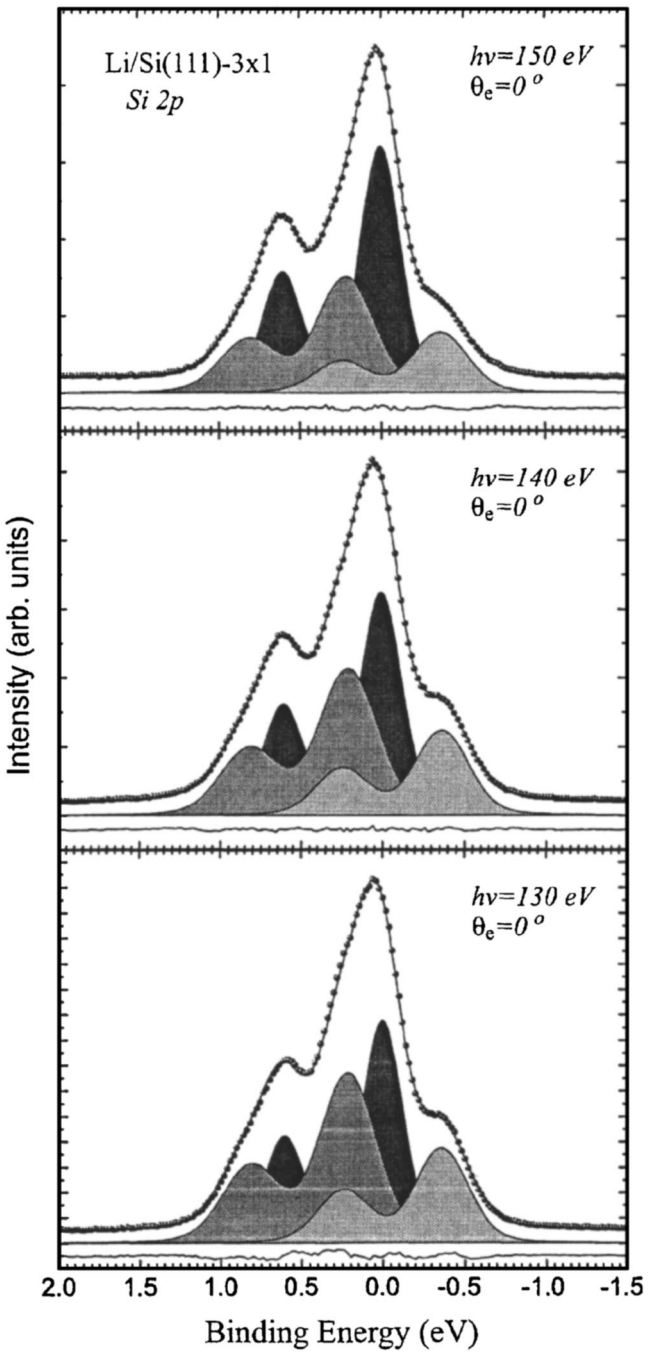

FIG. 2. Li/Si(111)-3×1 Si 2*p* core level spectra taken at several photon energies. Experimental data is indicated by circles, fitting data is shown as a continuous line. Also shown are the individual doublets, representing bulk, (black), and surface components, S_1 (light grey) and S_2 (grey). Binding energies are referenced to the bulk position. Finally, the residual between experimental and fitted data is included under each spectra. (The background has been removed prior to display.)

photon energies of ≈130 eV. Increasing the emission angle further increases surface sensitivity. Photon energies higher and lower than 130 eV yield more bulk sensitive spectra.

Data analysis was performed by least-square fitting of convoluted Gaussian and Lorentzian peak shapes (so-called Voigt profiles) to the experimental core-level data. Peaks that originate from the Si 2*p* orbitals have a spin-orbit split with a theoretical branching ratio of 2:1 giving rise to doublets. Shirley-type backgrounds were removed prior to fitting (when applicable). A summary of the fitting parameters for all reconstructions studied herein can be found in Table II.

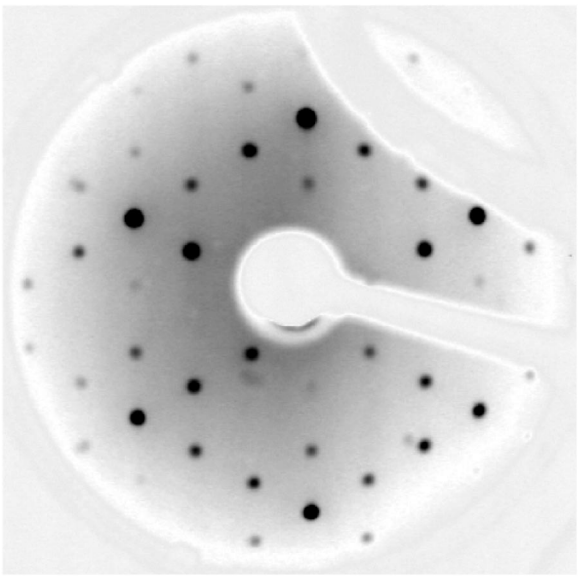

FIG. 3. Na/Si(111)-3×1 LEED image taken at 65 eV. Similar LEED patterns were observed for both Li and K.

A. Li/Si(111)-3×1

The Li/Si(111)-3×1 surface was prepared by evaporation of about 1.5 ML (1 ML=7.83×10^{14} atoms/cm^2) Li onto a gently heated surface, with 2 min postanneal (about 200–300 °C). The quality of the surface was checked by LEED and core-level spectra, showing sharp line shapes. The Li 1*s* spectrum (not shown) displayed only one component.

Si 2*p* core-level spectra from the Li/Si(111)-3×1 surface were taken using photon energies 120, 130, 140, and 150 eV. A collection of spectra is shown in Fig. 2, together with the results of the curve fitting procedure and the residual.

The experimental Si 2*p* data could be fitted by means of two surface related doublets lying at either side of the bulk Si $2p_{3/2}$ peak. The peak at lower binding energy, S_1, is shifted −0.36 eV with respect to the bulk. A shift of 0.22 eV was found for the higher energy peak, S_2. These values can be compared to a previous study by Weitering, Shi, and Erwin[18] in which the shifts for the S_1 and S_2 components were −0.4 and 0.46 eV, respectively.

The Lorenztian full width at half maximum (FWHM) was kept constant at 85 meV. The bulk peak Gaussian FWHM was found to be 247 meV. The lower and higher shifted surface peaks, S_1 and S_2, were found to have a Gaussian FWHM of 332 meV and 368 meV, respectively. The ratio between the two surface components was found to be approximately 1:2.

B. Na/Si(111)-3×1

Surface preparation of the Na/Si(111)-3×1 surface was achieved by depositing Na while heating the sample to a

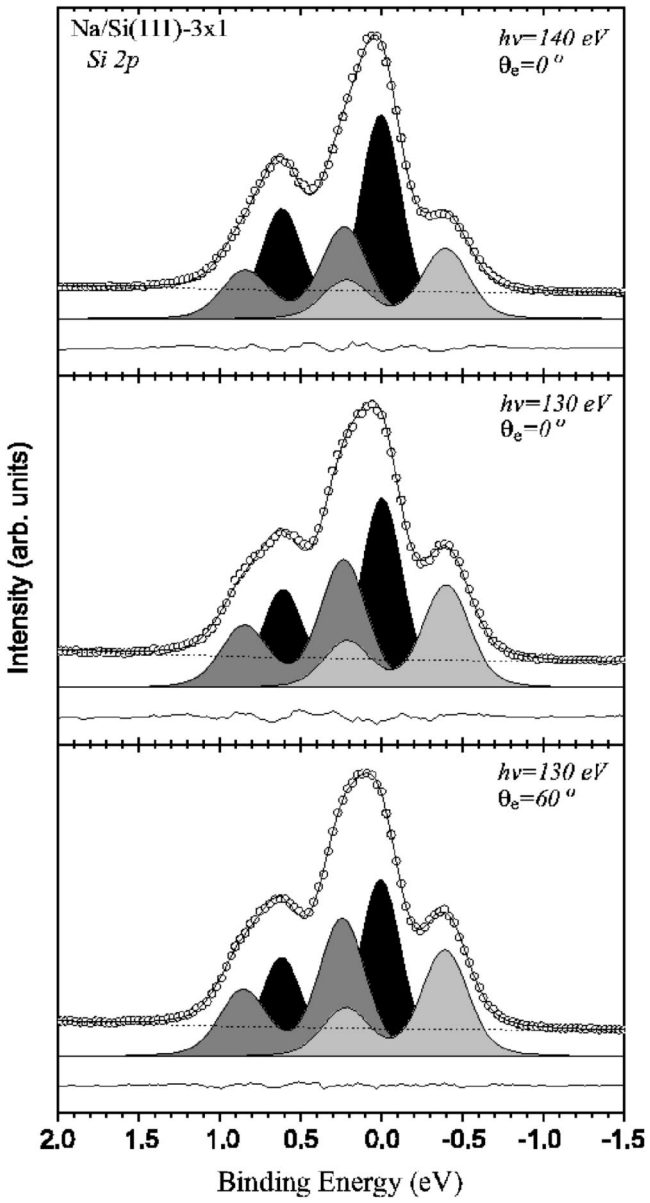

FIG. 4. Na/Si(111)-3×1 Si 2*p* core-level spectra taken at various photon energies. Experimental data is indicated by spheres, fitting data is shown as a continuous line. Also shown are the individual doublets, representing bulk, (black), and surface components, S_1 (light grey) and S_2 (grey). Binding energies are referenced to the bulk position. Finally, the residual between experimental and fitted data is included under each spectra.

temperature of 500 °C. This resulted in a three-domain 3 ×1 surface, as seen in LEED (shown in Fig. 3). A number of Si 2*p* core-level spectra at photon energies between 115 eV and 150 eV were taken. The sample was cooled using liquid nitrogen during measurements to minimize phonon broadening. A collection of the spectra is shown in Fig. 4. The spectra could be fitted using one bulk component (black) and two surface components, S_1 (light grey), and S_2 (grey).

The shifts for the two surface components, S_1, and S_2, with respect to the main bulk Si 2*p* component were found to be −0.40 eV and 0.24 eV, respectively. The Lorentzian FWHM was kept constant at 85 meV. The Gaussian broadening of the bulk component was found to be 248 meV, whereas the surface components were found to be 290 meV and 294 meV for S_1 and S_2, respectively. The residual between the experimental data and the fitted curve is also shown in Fig. 4. The intensity ratio between the two surface components was found to be approximately 1:1.25 (S_2 was slightly larger than S_1). We note that the S_2 component for both the Li/Si(111)-3×1 and Na/Si(111)-3×1 reconstructions have similar shifts, whereas the S_1 component has shifted to lower binding energy in the case of Na.

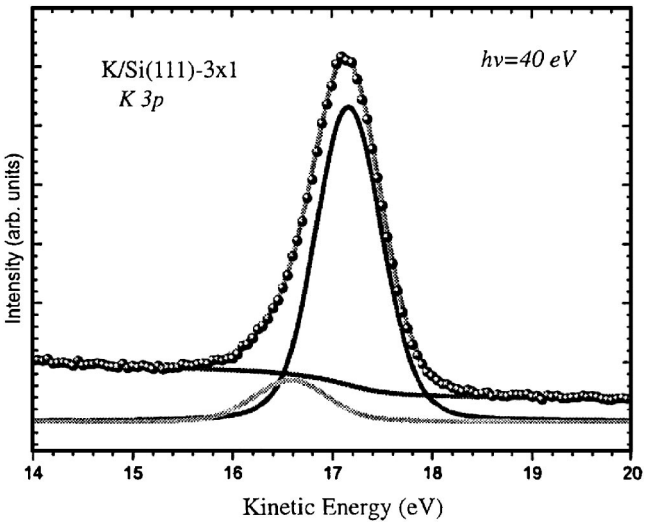

FIG. 5. (Color online) Experimentally obtained K 3*p* core-level spectrum taken at 40 eV. Experimental data is indicated by spheres, fitting data are shown as a continuous line. A smaller second peak is present in the spectrum.

C. K/Si(111)-3×1

The K/Si(111)-3×1 surface was obtained in a similar way as for Na. During the 5 min K deposition, and for a short time after the deposition was stopped, the sample was heated to a temperature of 500 °C. The quality of the surface was checked using LEED and core-level spectra of the K 3*p* peak. LEED showed a well defined three-domain 3×1 pattern similar to that shown in Fig. 3. The K 3*p* core-level spectra showed a dominant single peak, but also a small second peak at higher binding energy, as seen in Fig. 5.

A number of Si 2*p* core-level spectra at photon energies between 115 eV and 150 eV were taken. A collection of Si 2*p* core-level data taken at various photon energies is shown in Fig. 6. In addition, valence band spectra were recorded (not shown). The sample was cooled using liquid nitrogen during measurements to minimize phonon broadening.

Fitting of the experimental data was achieved using one spin-orbit split doublet from the bulk, *B*, and three surface related doublets, S_1, S_2, and S_3. These were found to lie at a distance of −0.57 eV, 0.25 eV, and 0.57 eV from the main bulk Si $2p_{3/2}$ peak. Once again, we find that the S_2 component is similar to the previous cases. The S_1 component was found to shift to a lower binding energy than both the Li and Na induced Si(111)-3×1 reconstructions. The height ratios

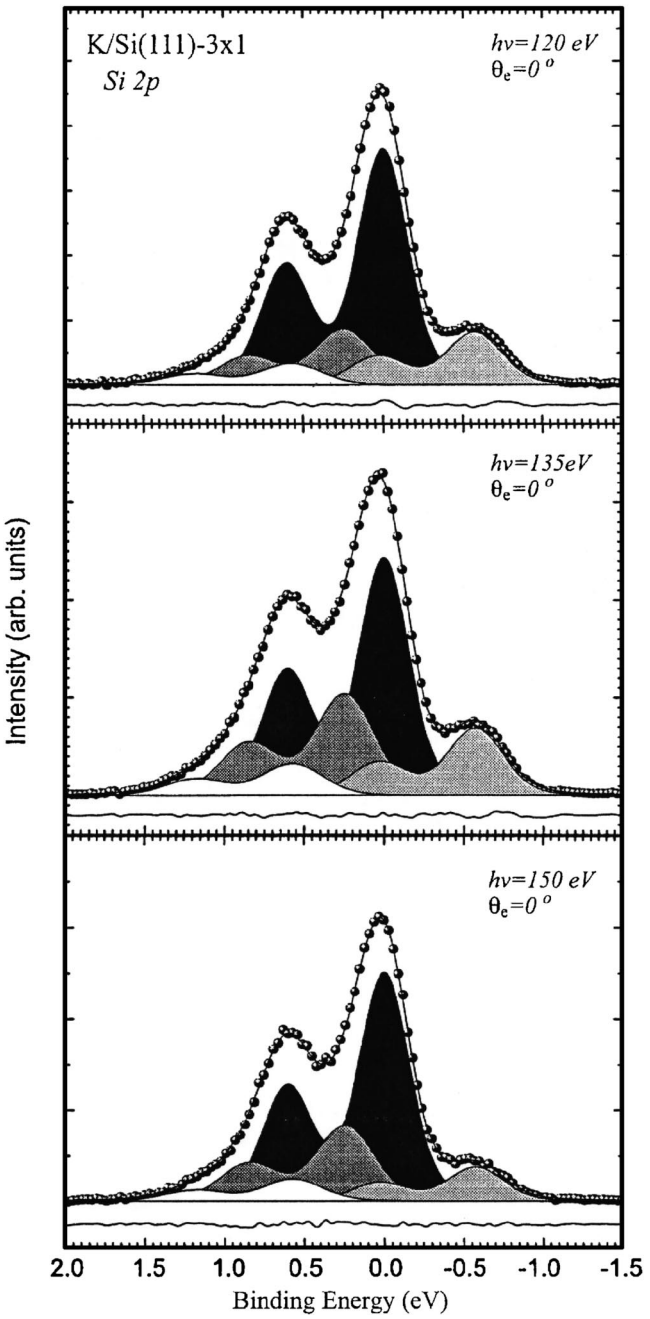

FIG. 6. K/Si(111)-3×1 Si 2*p* core-level spectra taken at various photon energies. Experimental data are indicated by spheres, fitting data is shown as a continuous line. Also shown are the individual doublets, representing bulk, (black), and surface components, S_1 (light grey), S_2 (grey), and S_3 (white). Binding energies are referenced to the bulk position. Finally, the residual between experimental and fitted data is included under each spectra. Contributions from the background have been removed.

between the S_1 and S_2 components was ascertained to be approximately 1:1.2. Most notable in the K/Si(111)-3×1 Si 2*p* core-level spectra is the requirement of an additional surface component, S_3, to obtain a consistent fit. An additional component was also observed in the K 3*p* core-level spectra (see Fig. 5). This component was observed to decrease when gently heating the sample. A similar component in the Na 2*p*

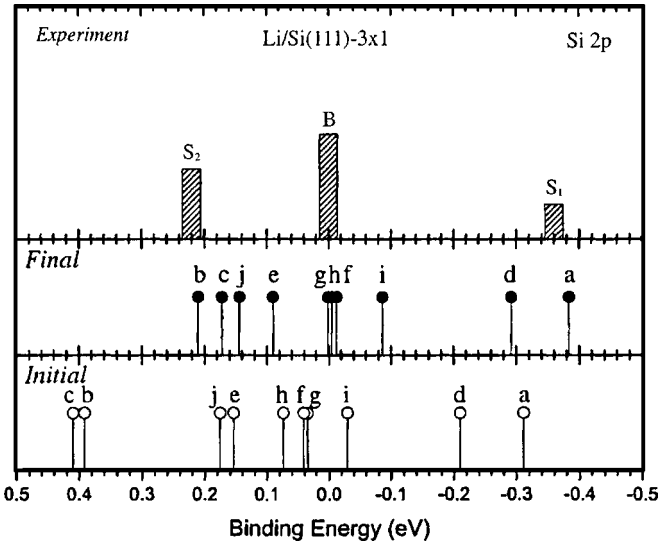

FIG. 7. Calculated core-level shifts for both initial (open circles) and final-state effect (filled circles) schemes for the three uppermost layers for the Li/Si(111)-3×1 reconstruction. Energies are referenced to the bulk core-level energy.

spectra has been discussed by Paggel *et al.*[21] for the case of the Na/Si(111)-3×1 reconstruction and was attributed to the presence of Na in a precursor state on the surface. This peak was also seen by Paggel *et al.* to decrease when heating gently.

V. DISCUSSION

For the honeycomb chain-channel model, one would expect four Si 2*p* surface components that are derived from the top layer. These surface components would originate from the alkali metal bonded Si atoms, *a* and *d*, and the Si double bonded atoms, *b* and *c*. Surface components may also originate from the second and third layers (see Fig. 1).

It is however, by no means certain that all of these surface related peaks can be resolved due to the relatively small differences in core-level shifts between them. This was found to be the case here for the Li, Na, and K induced Si(111)-3×1 reconstructions, in which only two surface related components, S_1 and S_2, were found for Li and Na, and three for K.

With the exception of the S_3 component found in the core-level spectra for K/Si(111)-3×1, all three spectra series are strikingly similar. This is a strong indication that the alkali metals, Li, Na, and K do indeed share a common Si(111)-3×1 reconstruction.

In all three cases we observe a lower binding energy component, S_1, which is well separated from the main bulk component. Furthermore, from the summary of fitting parameters (Table II) it becomes evident that as the size of the alkali atom increases, so does the shift of S_1 away from the main bulk component to lower binding energies. The fact that the S_1 component clearly depends on the alkali metal adatom size suggests that this component derives from the alkali bonded Si atoms, *a* and *d*. On the higher binding energy side

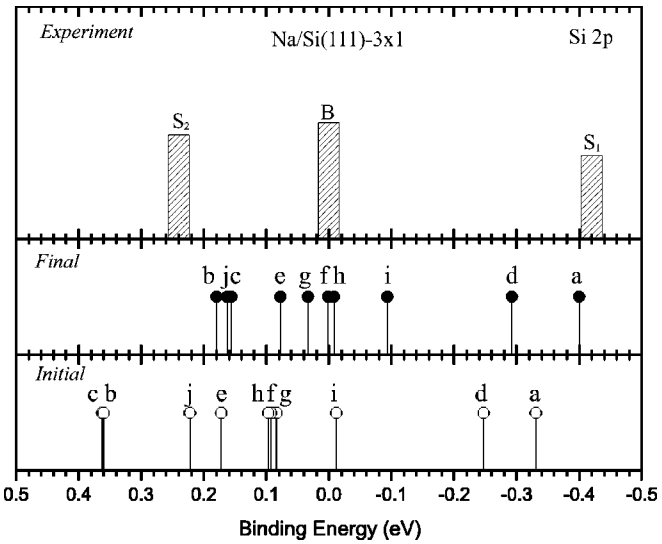

FIG. 8. Calculated core-level shifts for both initial (open circles) and final-state effect (filled circles) schemes for the three uppermost layers for the Na/Si(111)-3×1 reconstruction. Energies are referenced to the bulk core-level energy.

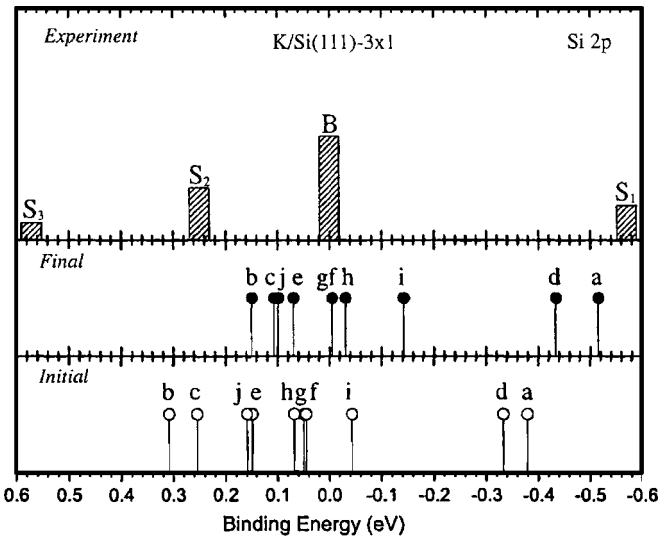

FIG. 9. Calculated core-level shifts for both initial (open circles) and final-state effect (filled circles) schemes for the three uppermost layers for the K/Si(111)-3×1 reconstruction. Energies are referenced to the bulk core-level energy.

of the main bulk component we observe a surface component, S_2, which is located at approximately the same energy for all three cases. However, the intensity ratio between this peak and the S_1 component was found to vary for the three reconstructions. Identification of the origin of the S_2 component based on experiment is problematic, since one expects contributions from several atoms in this spectral range. The relatively broad components for the alkali adatom cases also allows for composite peaks. Especially the Li case, with an anomalously high intensity for S_2, clearly suggest contributions from several atoms. Nevertheless the dominant contribution is expected to come from the double bonded top Si atoms, *b* and *c*.

A. Li/Si(111)-3×1

Results from DFT calculations using both initial and final-state schemes together with the experimentally determined SCLS can be seen in Fig. 7. Initial state calculations show shifts of −0.18 and −0.28 eV for the alkali bonded Si atoms. This confirms our assignment of the S_1 component. The calculated values are however underestimated compared to the experimentally found shift for the S_1 component which was found to be −0.36 eV. On the high energy side, the two core-level energies related to the double bond are found at approximately 0.4 eV above the bulk, which can be compared to the S_2 component which was found to lie at 0.22 eV. The 1:2 intensity ratio of the two surface components, S_1 and S_2, is inconsistent with the HCC model assuming that the peaks originate from the first layer alkali bonded and double bonded Si atoms. The cause of this discrepancy could be a photoelectron diffraction effect. However, a more likely explanation would be a superposition of several peaks at the S_2 position.

With the introduction of final-state effects in the calculations, one observes significant differences in the SCLS, especially on the high binding energy side. Here one observes that the double bonded atoms *b* and *c* move down in binding energy coming closer to the energies for atoms *e* and *j*. The gap between energies reduces to a point in which the lower energy double bonded atom is only 0.03 eV larger that the third layer channel atom *j*. Also, the dangling bond Si atom, *e*, is found to lie in proximity to the double bond energies (0.08 eV lower energy). The clustering of these core-levels may explain the experimentally obtained data with a ratio of 1:2 between S_1 and S_2. This would indicate that the S_2 component is a composite peak with contributions from four different atoms. Similar effects and differences between calculations for initial and final-state schemes have been reported by Baski *et al.*[10] for the Ca/Si(111)-3×1 reconstruction.

B. Na/Si(111)-3×1

A look at the experimental Na/Si(111)-3×1 core-level data (Fig. 4) shows two surface components with relative peak heights between the two components of approximately 1:1.25. This would be more consistent with surface components that originate from the alkali bonded Si atoms and from the double bonded Si atoms only compared to that of the Li induced Si(111)-3×1 reconstruction. The heights of the two surface components both show similar changes with variations of the surface sensitivity of the measurements. This is an indication again that both components derive from the same layer. Density functional theory calculations both using initial and final-state schemes show that the S_1 component at lower binding energy derives from the alkali bonded Si atoms *a* and *d* (shown in Fig. 8). Initial state calculations show two almost identical eigenvalues for the double bonded top layer atoms *b* and *c* at 0.35 eV. The alkali bonded atoms were found to have initial state energies of −0.26 and −0.35 eV, respectively. These values are comparable to previous calculations by Kang, Kang, and Jeong.[7]

By inclusion of final-state effects, the eigenvalues for atoms *b* and *c* move down and the energy of atom *j* increases causing overlap of the energies. This additional component is consistent with the variation from a 1:1 ratio for the two surface components, S_1 and S_2, in the Na induced Si(111)-3×1 reconstruction

C. K/Si(111)-3×1

Initial state calculations for the K/Si(111)-3×1 reconstruction show two core-level components from the two alkali bonded Si atoms, *a* and *d*, at −0.38 and −0.33 eV, respectively (see Fig. 9). The shifts are observed to be larger than both the Li and Na induced reconstructions and as such is consistent with the observed trend for the experimentally obtained S_1 surface component. However, as was the case for both the Li and Na induced reconstructions, this shift is underestimated. On the high binding energy side initial state calculations show two double bonded components, *b* and *c*, at 0.31 and 0.25 eV respectively. At approximately 0.15 eV we find the SCLS for the atoms *e* and *j*. Final-state calculations show a similar picture to that of the Li/Si(111)-3×1 final-state calculations, in which both the channel atom *j*, and the dangling bond atom, *e*, move closer in energy to the double bonded atoms, *b* and *c*, giving rise to core-levels with significant energy overlap. One can, based on the final-state calculations, conclude that the S_2 component is a composite of the double bonded Si atoms, *b* and *c*, together with the dangling bond atom *e*, and the atom *j* situated at the bottom of the channel. This assignment is consistent with the observed height ratio between the S_1 and S_2 surface components. Differences in the height ratios between the Li and K induced reconstructions may be explained by the larger size of the K adatom suppressing emission from the *j* atoms situated at the bottom of the channel to a greater extent than for the case of the Li adatoms.

However, one surface component does not appear in either the initial or final-state calculations, and that is the S_3 component. We therefore conclude, based on DFT calculations for the HCC model, that this surface component is not consistent with the HCC model, and could therefore be related to imperfections in the surface structure.

VI. CONCLUSION

In conclusion, we have studied the surface core-level shifts, using synchrotron radiation, for the *M*/Si(111)-3×1 reconstruction for *M*=Li, Na, and K. The alkali induced Si(111)-3×1 reconstructions were found to have at least two surface related components, S_1 and S_2. Density functional theory calculations have also been performed using both initial and final-state schemes to determine core-level shifts for these reconstructions based on the HCC model. Trends in the energy of the S_1 component show shifts to lower binding energies with respect to the main bulk component with increasing alkali metal size. This trend was found to be emulated by both the initial and final-state scheme calculations. We therefore conclude that S_1 does indeed originate from the alkali bonded Si atoms, *a* and *d*.

The origin of the S_2 component is more complicated. Based on the ratios between the S_1 and S_2 components we conclude that the S_2 component derives from a number of atoms and not simply from the top layer double bonded Si atoms, *b* and *c*. Li/Si(111)-3×1 final-state calculations show four atoms with energies in close proximity to each other. All of these atoms may contribute to the S_2 component. We therefore conclude that for the Li induced Si(111)-3×1 reconstruction, the S_2 component derives from the double bonded Si atoms, *b* and *c*, together with the dangling bond Si atom *e* and channel atom *j*.

In the case of the Na induced Si(111)-3×1 reconstruction we propose that the S_2 component derives mainly from the double bonded Si atoms, *b* and *c*, with additional contributions from atom *j* situated at the bottom of the channel and possibly atom *e*.

Also for the K induced surface we observed, in the final-state calculations, an additional two atoms from which the S_2 component may derive besides the two double bonded Si atoms, namely atoms *e* and *j*.

By inclusion of final-state effects, the calculated SCLS were found to be in fairly good agreement with the experimental results, especially for the S_1 component. The S_2 component is less well reproduced using final-state DFT calculations. The small shift to larger binding energy of the S_2 component with increasing alkali size was not seen in either the initial or final-state DFT calculations, although final-state DFT calculations were found to show a more quantitative agreement with experiment than those calculations based solely on initial-state calculations.

ACKNOWLEDGMENTS

The authors would like to thank the staff at the Max-lab facility and in particularly T. Balasubramanian. The work done here was funded by the Swedish Research Council.

*Electronic address: Lars.Johansson@kau.se

[1] S. C. Erwin, Phys. Rev. Lett. **75**, 1973 (1995).
[2] H. H. Weitering, N. J. DiNardo, R. Pérez-Sandoz, J. Chen, and E. J. Mele, Phys. Rev. B **49**, 16837 (1994).
[3] G. C. L. Wong, C. A. Lucas, D. Loretto, A. P. Payne, and P. H. Fuoss, Phys. Rev. Lett. **73**, 991 (1994).
[4] C. Collazo-Davila, D. Grozea, and L. D. Marks, Phys. Rev. Lett. **80**, 1678 (1998).
[5] L. Lottermoser, E. Landemark, D. M. Smilgies, M. Nielsen, R. Feidenhans'l, G. Falkenberg, R. L. Johnson, M. Gierer, A. P. Seitsonen, H. Kleine *et al.*, Phys. Rev. Lett. **80**, 3980 (1998).
[6] S. C. Erwin and H. H. Weitering, Phys. Rev. Lett. **81**, 2296 (1998).
[7] M. H. Kang, J. H. Kang, and S. Jeong, Phys. Rev. B **58**, R13359

(1998).
[8] K. Sakamoto, H. Ashima, H. M. Zhang, and R. I. G. Uhrberg, Phys. Rev. B **65**, 045305 (2001).
[9] M. Gurnett, J. B. Gustafsson, K. O. Magnusson, S. M. Widstrand, and L. S. O. Johansson, Phys. Rev. B **66**, 161101(R) (2002).
[10] A. A. Baski, S. C. Erwin, M. S. Turner, K. M. Jones, J. W. Dickinson, and J. A. Carlisle, Surf. Sci. **476**, 22 (2001).
[11] T. Okuda, H. Ashima, H. Takeda, K. S. An, A. Harasawa, and T. Kinoshita, Phys. Rev. B **64**, 165312 (2001).
[12] G. Lee, S. Hong, H. Kim, D. Shin, J.-Y. Koo, H.-I. Lee, and DaeWon Moon, Phys. Rev. Lett. **87**, 056104 (2001).
[13] J. Schäfer, S. C. Erwin, M. Hansmann, Z. Song, E. Rotenberg, S. D. Kevan, C. S. Hellberg, and K. Horn, Phys. Rev. B **67**, 085411 (2003).
[14] J. Y. Lee and M. H. Kang, Phys. Rev. B **66**, 233301 (2002).
[15] T. Okuda, K. Sakamoto, H. Nishimoto, H. Daimon, S. Suga, T. Kinoshita, and A. Kakizaki, Phys. Rev. B **55**, 6762 (1997).
[16] K. S. An, R. J. Park, J. S. Kim, C. Y. Park, C. Y. Kim, J. W. Chung, T. Abukawa, S. Kono, T. Kinoshita, A. Kakizaki *et al.*, Surf. Sci. Lett. **337**, L789 (1995).
[17] K. Sakamoto, T. Okuda, H. Nishimoto, H. Daimon, S. Suga, T. Kinoshita, and A. Kakizaki, Phys. Rev. B **50**, 1725 (1994).
[18] H. H. Weitering, X. Shi, and S. C. Erwin, Phys. Rev. B **54**, 10585 (1996).
[19] T. Okuda, H. Shigeoka, H. Daimon, S. Suga, T. Kinoshita, and A. Kakizaki, Surf. Sci. **321**, 105 (1994).
[20] J. J. Paggel, H. Haak, W. Theis, and K. Horn, J. Vac. Sci. Technol. B **11**, 1439 (1993).
[21] J. J. Paggel, G. Neuhold, H. Haak, and K. Horn, Phys. Rev. B **52**, 5813 (1995).
[22] B. Jensen, S. Butorin, T. Kaurila, R. Nyholm, and L. Johansson, Nucl. Instrum. Methods Phys. Res. A **394**, 243 (1997).
[23] A. Ishizaka and Y. Shiraki, J. Electrochem. Soc. **133**, 666 (1986).
[24] D. Y. Petrovykh, K. N. Altmann, J. L. Lin, F. J. Himpsel, and F. M. Leibsle, Surf. Sci. **512**, 269 (2002).
[25] O. Gallus, T. H. Pillo, P. Starowicz, and Y. Baer, Europhys. Lett. **60**, 903 (2002).
[26] Y. K. Kim, J. W. Kim, H. S. Lee, Y. J. Kim, and H. W. Yeom, Phys. Rev. B **68**, 245312 (2003).
[27] P. Blaha, K. Schwarz, G. K. H. Madsen, D. Kvasnicka, and J. Luitz, WIEN2K, An Augmented Plane Wave Plus Local Orbitals Program for Calculating Crystal Properties (2001), ISBN 3-9501031-1-2.
[28] J. P. Perdew, K. Burke, and M. Ernzerhof, Phys. Rev. Lett. **77**, 3865 (1996).
[29] J. F. Janak, Phys. Rev. B **18**, 7165 (1978).
[30] Image of the honeycomb chain-channel model created using AtomEye, J. Li, Modell. Simul. Mater. Sci. Eng. **11**, 173 (2003).